cmgh
CELLULAR AND MOLECULAR GASTROENTEROLOGY AND HEPATOLOGY

ORIGINAL RESEARCH

Highly Sensitive, Flow Cytometry-Based Measurement of Intestinal Permeability in Models of Experimental Colitis

Kevin Tsai,[1,2] Caixia Ma,[2] Xiao Han,[2] Joannie Allaire,[2] Genelle R. Lunken,[2] Shauna M. Crowley,[2] Hongbing Yu,[2] Kevan Jacobson,[1,2] Lijun Xia,[3] John J. Priatel,[1,4] and Bruce A. Vallance[1,2]

[1]British Columbia Children's Hospital Research Institute, Vancouver, British Columbia, Canada; [2]Department of Pediatrics, University of British Columbia, Vancouver, British Columbia, Canada; [3]Cardiovascular Biology Research Program, Oklahoma Medical Research Foundation, Oklahoma City, Oklahoma; and [4]Department of Pathology and Laboratory Medicine, University of British Columbia, Vancouver, British Columbia, Canada

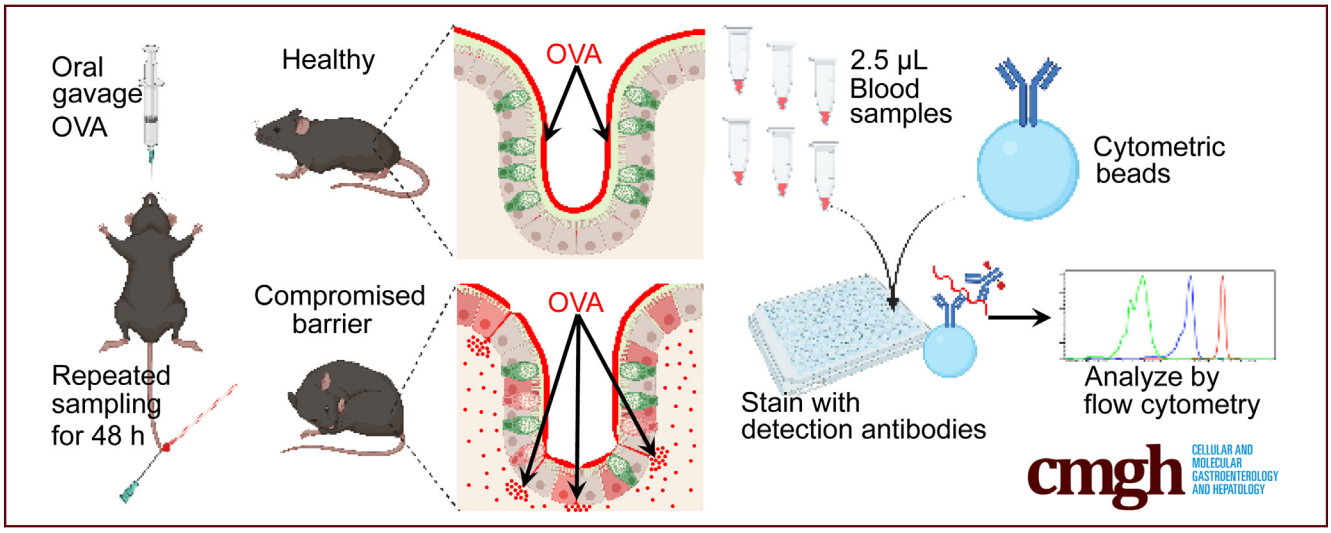

SUMMARY

We show that a flow cytometry–based assay of orally gavaged ovalbumin passage via the gut and into the plasma provides great sensitivity and utility for the measurement of intestinal permeability in experimental models of intestinal infection and colitis.

BACKGROUND & AIMS: Increased intestinal permeability is seen in a variety of inflammatory conditions such as enteric infections and inflammatory bowel disease. Because barrier function can provide a key biomarker of disease severity, it often is assayed in animal models. A common methodology involves gavaging mice with fluorescein isothiocyanate–conjugated dextran (FITC-D), followed by cardiac puncture to assay plasma fluorescence on a spectrophotometer. Although the FITC-D method is relatively simple, its sensitivity is limited and enables only a single measurement because the test requires killing the subject. Herein, we describe a novel flow cytometry–based method of intestinal permeability measurement based on detection of orally gavaged ovalbumin (OVA) that leaks out of the gut. Our approach uses minute blood volumes collected from the tail vein, permitting repeated testing of the same subject at multiple time points. By comparing this assay against the gold standard FITC-D method, we show the expanded utility of our OVA assay in measuring intestinal permeability.

METHODS: We directly compared our OVA assay against the FITC-D assay by co-administering both probes orally to the same animals and subsequently using their respective methodologies to measure intestinal permeability by detecting probe levels in the plasma. Permeability was assessed in mice genetically deficient in intestinal mucus production or glycosylation. In addition, wild-type mice undergoing dextran sodium sulfate–induced colitis or infected by the enteric bacterial pathogen *Citrobacter rodentium* also were tested.

RESULTS: The OVA assay showed very high efficacy in all animal models of intestinal barrier dysfunction tested. Besides identifying intestinal barrier dysfunction in mice with impaired mucin glycosylation, the assay also allowed for repeated tracking of intestinal permeability within the same animal over time, providing data that cannot be easily acquired with other currently applied methods.

CONCLUSIONS: The OVA assay is a highly sensitive and effective method of measuring intestinal permeability in mouse models of barrier dysfunction and experimental colitis. *(Cell Mol Gastroenterol Hepatol 2023;15:425–438; https://doi.org/10.1016/j.jcmgh.2022.10.004)*

Keywords: Cytometric Bead Assay; Intestinal Permeability Assay; ELISA; Leaky Gut; Inflammatory Bowel Disease.

The gastrointestinal (GI) tract is lined by a single layer of intestinal epithelial cells (IECs), that provide several key functions such as nutrient absorption and the secretion of antimicrobial peptides and mucins.[1] The mucus barrier overlying the IECs is produced by goblet cells (an IEC subset) and is largely composed of the highly glycosylated mucin-2 (Muc2) that is released apically into the intestinal lumen.[1] Together, the epithelial and mucus layers form a semipermeable, protective mucosal barrier that allows for nutrient absorption while also segregating luminal microbes away from the epithelium to limit their contact with the epithelial lining. Correspondingly, any perturbation to the structure or function of this mucosal barrier resulting from genetic mutations or noxious dietary or microbial factors may result in the leakage of luminal contents (microbes, microbial products, dietary antigens) out of the GI tract, and cause acute activation of the underlying immune system. Such leakage can lead to local immune cell activation, further damage to the mucosal barrier, and, in some cases, chronic inflammation or even sepsis, as seen in patients with inflammatory bowel disease (IBD).[2,3]

Intestinal permeability, commonly defined as the measurable diffusion rate of luminal contents across the mucosal barrier into the circulation, is the parameter typically used to assess the integrity of the intestinal mucosal barrier.[4–6] Recent studies have shown that increased intestinal permeability precedes Crohn's disease, and often is associated with the development of this form of IBD.[7] Moreover, increased intestinal permeability can serve as a biomarker for disease activity in IBD patients.[8–11] In addition to IBD, significant increases in intestinal permeability have been associated with heightened susceptibility to a variety of autoimmune conditions such as type 1 diabetes, systemic lupus erythematosus, rheumatoid arthritis, and multiple sclerosis.[12–14] Consequently, the importance of intestinal permeability in these pathologic conditions highlights its potential use as a biomarker for early detection of disease activity and/or disease relapse.

Aside from their applicability in the clinic, intestinal permeability measurements also commonly are used with preclinical models.[4,5] Current methodologies can be broadly divided into 2 categories. The first involves the detection of orally ingested probe(s) in the blood or urine, with lactulose/mannitol or ^{51}Chromium measured in patients, while fluorescein isothiocyanate–conjugated dextran (FITC-D) is commonly used in mouse models of intestinal barrier dysfunction.[4,6] These approaches permit an in vivo assessment of the GI tract as a whole. By contrast, the second category relies on an ex vivo assessment of electrical conductivity across excised intestinal tissues (Ussing chambers).[15] Although these methods are highly useful for measuring intestinal permeability, their cost, complexity, or invasiveness,[16,17] limits their broad applicability. Moreover, the FITC-D and Ussing chamber assays are both unable to measure intestinal permeability across multiple time points within the same animal or biospecimen.

In this report, we describe and validate a novel flow cytometry–based method to measure intestinal permeability in several well-characterized mouse models of intestinal inflammation and barrier dysfunction. By gavaging mice with chicken ovalbumin (OVA), and collecting tiny volumes of blood, we used immunoprecipitation-based flow cytometry to quantitate OVA in their plasma at a sensitivity level far surpassing the FITC-D method. Furthermore, there was no need to kill the test animals, allowing repeated measurements of intestinal permeability over several hours or days in the same animal. Because our methodology requires a minute fraction of the blood volume typically needed for standard permeability assays, and because the OVA probe, a common dietary protein, is relatively harmless, we believe our approach is a strong candidate for future adaptation to the clinic.

Results

The Construction, Validation, and Workflow of the Cytometric Bead Assay

The OVA assay protocol uses antibody-conjugated carboxylate modified (CML) beads to capture the probe antigen OVA (Figure 1*A*–*D*). To perform the assay, the animal was first gavaged with 1 mg OVA suspended in 100 μL phosphate-buffered saline (PBS). Heparin-coated capillary tubes were premarked to ensure sampling consistency (Figure 1*C*), and, as indicated in Figure 1*D*, they were used to collect 2.5 μL blood by poking the tail with a 25-gauge needle. Blood cells within the samples were first lysed with 10 μL Tween 20 containing fluorescence-activated cell sorter buffer, cellular debris was removed by centrifugation at 3000 $\times$ *g* for 5 minutes, and the supernatant then transferred into a 96 well U-bottom plate. The OVA-specific CML beads were added to the blood samples and incubated at 4°C on a plate shaker. The OVA–CML bead complexes were pelleted via centrifugation and detected using a rabbit anti-OVA polyclonal antibody in conjunction with

Abbreviations used in this paper: **CML, carboxylate modified latex; DSS, dextran sulfate sodium salt; EDAC, 1-ethyl-3-(3-dimethylaminopropyl) carbodiimide; F(ab)$_2$, divalent antibody fragments; FACST, 1× PBS, 2% heat inactivated fetal bovine serum, 2 mmol/L EDTA, and 0.05% Tween 20; FITC-D, fluorescein isothiocyanate–conjugated dextran; GI, gastrointestinal; IBD, inflammatory bowel disease; IEC, intestinal epithelial cell; LM, lactulose mannitol; MES, 2-(N-morpholino) ethanesulfonic acid; OVA, ovalbumin; PBS, phosphate-buffered saline; PE, phycoerythrin; pi, postinfection; WT, wild-type.**

Most current article

2352-345X
https://doi.org/10.1016/j.jcmgh.2022.10.004

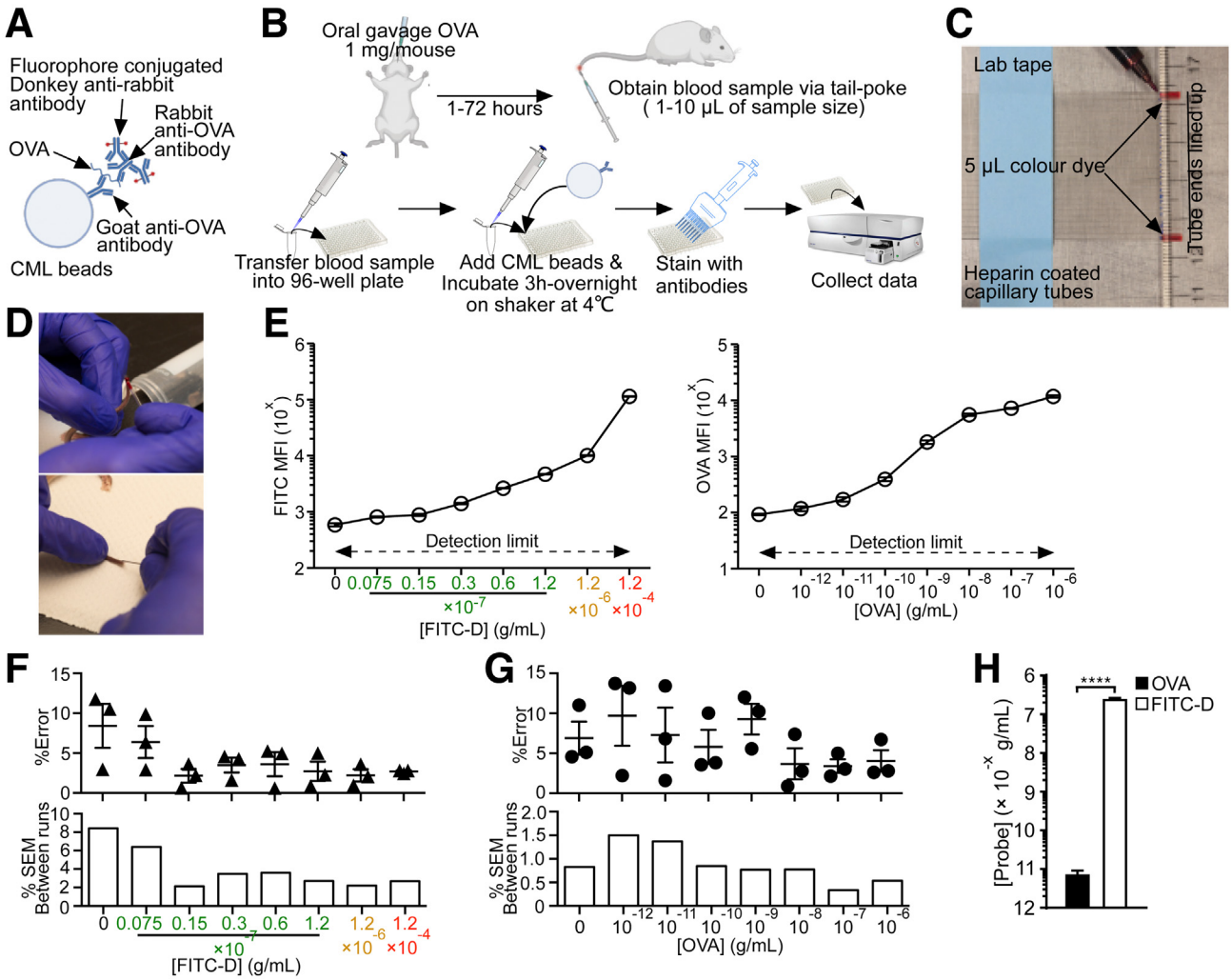

Figure 1. Components, workflow, and sensitivity of the OVA assay. (*A*) Principle of the OVA assay for intestinal permeability measurement by flow cytometry. (*B*) The workflow of the OVA assay. (*C*) Production of capillary tubes with a set volume for blood sampling. (*D*) A 25-gauge needle was used to puncture the tails of anesthetized mice for blood collection. The tail puncture was performed at a shallow angle, parallel to the tail as illustrated. Blood samples were collected using marked capillary tubes produced in panel *C*. (*E*) Comparison of dynamic ranges of the OVA and FITC-D assays using standard curves. Each data point represents a triplicate of readouts obtained from serially diluted probes of the respective assays. (*F*) Percentage error of 3 separate standard curve readouts of the OVA assay or FITC-D assay across all concentrations. The percentage error is calculated by dividing the SEM derived from a triplicate of readings by the average value of the triplicates. (*G*) Comparison of the errors between 3 separate experiments of panel *A* across all concentrations. SEM values were generated from the 3 separated percentage error values in panel *A* and plotted as bar graphs. (*H*) Comparison of the background noise of the respective assays (C57/BL6 mice, n = 4). MFI, mean fluorescent intensity. **** $P \leq .0001$.

phycoerythrin-conjugated donkey anti-rabbit IgG polyclonal $F(ab)_2$ fragments (preabsorbed to serum proteins of multiple species to minimize cross-reactivity to other Ig molecules).

To compare the sensitivity and dynamic range of the OVA assay with the FITC-D assay, we first compared the OVA standard curve with the FITC-D standard curve. The FITC-D assay has a dynamic range roughly from 10^{-3} to 10^{-8} g/mL of FITC-D whereas the OVA assay has a dynamic range from 10^{-6} to 10^{-12} g/mL of OVA (Figure 1*E*). The detection limit of the OVA assay (10^{-12} g/mL) suggests that the OVA assay is potentially far more sensitive than the FITC-D assay (Figure 1*E*). Next, we analyzed the amount of variance that existed within triplicate readings from standard curves of 3 separate experiments by comparing the percentage of error derived from the readings. We found the percentage error of the OVA assay was approximately 5% at all concentrations whereas the percentage error was higher, approximately 10%, at the lower concentrations of the FITC-D assay (Figure 1*F* and *G*, upper panel). We then analyzed the variance between each assay by comparing the variance of errors within these 3 separate experiments. We found that the OVA generated more consistent results across all concentrations as indicated by the less than 2% error between experiments compared with the FITC-D assay, which varied between 2% and 8% error (Figure *F* and *G*, lower panel).

Next, we compared the background signals of the respective assays by converting and comparing fluorescence values of the probe-free blood samples into their respective concentration values. We found that compared with the negligible background signal of the OVA assay, the FITC-D assay showed much higher background in the absence of the probe (Figure 1*H*) (OVA, 7.9×10^{-12} g/mL vs FITC-D, 2.6×10^{-7} g/mL). Taken together, these data suggest that the OVA assay is potentially more consistent and sensitive at measuring target concentrations and shows lower background noise compared with the FITC-D assay.

Orally Gavaged OVA Is Found Lining the Lumen Throughout the Distal GI Tract

We next sought to determine the localization of OVA postgavage. Healthy, female C57BL/6 mice, aged 6–10 weeks, were gavaged with 100 μL PBS solution containing 1 mg OVA. Based on our previous finding that OVA levels in the blood peaked at approximately 6 hours postgavage,[18] we killed mice at this time point, collecting their blood as well as small intestinal and colonic tissues. As expected for unmanipulated wild-type (WT) C57BL/6 mice,[18] minimal levels of OVA were detected in their plasma (1.2×10^{-12} g/mL; n = 4) (Figure 2*A*). We next stained formalin-fixed intestinal tissue sections using the same rabbit anti-OVA antibody used in the OVA assay. Very little, if any, OVA signal was found within the small intestine (duodenum, jejunum, and ileum) because this protein likely had passed into the distal GI tract by this time point, or had been digested into small undetectable fragments and absorbed (Figure 2*B*). By contrast, staining of the cecum and colon (proximal, medial, and distal) showed very strong OVA signals localized to the lumen and the mucosal surface (Figure 2*C*). These findings suggest that much of the orally gavaged OVA remained partially digested or undigested, passing out of the small intestine and localizing to the cecal and colonic lumen. Thus, the localization of gavaged OVA appears to be well suited to assess barrier function within the distal GI tract.

The OVA Assay Enables Sensitive Measurement of Gut Permeability During Dextran Sodium Sulfate Colitis

Based on the earlier-described findings, we chose the dextran sodium sulfate (DSS) model of colitis to further investigate the utility of our OVA assay in measuring intestinal permeability. The model reflects the ability of DSS to act as a chemical irritant on the colonic epithelium, with the resulting damage precipitating colitis and increasing intestinal permeability.[19] We first treated cohorts of female

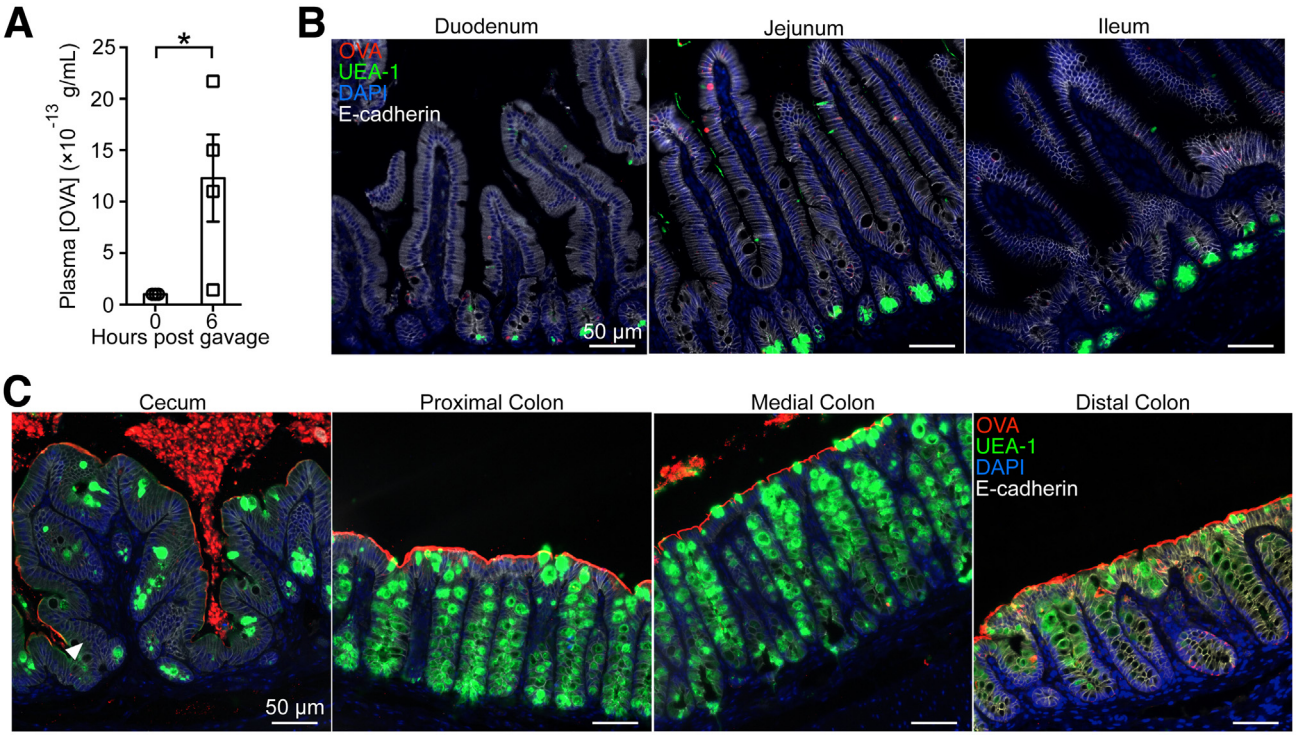

Figure 2. Detection of the OVA protein within blood and various regions of the GI tract. (*A*) OVA concentrations detected in blood samples of C57BL/6 mice (n = 4), either before or 6 hours postgavage with 1 mg OVA. (*B*) Visualization of OVA localization in the small intestine. Histology samples were obtained from the earlier-mentioned mice, processed, and then stained for OVA (red), as well as intestinal epithelium (E-cadherin, white), fucosylated residues of mucin granules of goblet cells (Ulex Europaeus Agglutinin I [UEA-1] lectin, green), and nuclei (DAPI, blue). (*C*) Visualization of OVA localization in the cecum and colon. Histology samples were obtained from the same mice outlined in panels *A* and *B*, processed, and then stained as outlined for panel *B*. DAPI, 4′,6-diamidino-2-phenylindole. *$P \leq .05$

C57BL/6 mice with 3% DSS in their drinking water to damage their mucosal barrier and increase intestinal permeability.[20] On day 3 or day 6 of DSS exposure, subsets of mice were gavaged with 100 μL PBS solution containing 1 mg OVA and 12 mg FITC-D. Mice then were killed 3 or 6 hours postgavage to collect their blood via cardiac puncture. The amount of FITC-D present within the blood then was assessed immediately, using a fluorimeter, whereas OVA was measured using the OVA assay.

We found that both methods detected statistically significant increases in barrier permeability in the colitic mice over that of healthy untreated controls. Baseline FITC-D levels ($5.07 \pm 0.86 \times 10^{-7}$ g/mL) doubled to $1.78 \pm 0.31 \times 10^{-6}$ by day 3 DSS, and doubled again to $1.06 \pm 0.10 \times 10^{-6}$ by day 6 of colitis. Meanwhile, the increases in permeability were even easier to detect with the OVA assay, with the baseline signal of $2.50 \pm 0.43 \times 10^{-11}$ g/mL increasing by 100-fold to $2.62 \pm 1.24 \times 10^{-9}$ on day 3 of DSS, and a further 15-fold increase to $3.90 \pm 1.04 \times 10^{-8}$ by day 6 (Figure 3*A*). This is in keeping with previous observations that extended exposure to DSS leads to greater intestinal pathology and barrier dysfunction.[21] Notably, the OVA assay could detect statistically significant changes between the day 3 and day 6 DSS-treated groups with great confidence ($P = .0004$), whereas the FITC-D assay could not ($P = .13$) (Figure 3*A*). Thus, the OVA assay is at least as sensitive as the FITC-D assay in discriminating varying degrees of barrier dysfunction induced by DSS treatment.

Because these results indicate that OVA can readily cross the mucosal barrier in DSS-treated mice, we sought to visualize its translocation by immunofluorescence. We stained formalin-fixed distal colon sections from OVA gavaged (control or DSS-treated) mice as outlined earlier. We confirmed that in untreated WT mice, OVA lined the apical surface of the colonic epithelium, with no indication that it crossed the intact epithelial barrier (Figure 3*B*, upper panel). By contrast, this outline of the mucosal surface was no longer observed in OVA gavaged, DSS-treated mice (Figure 3*B*, lower panel). Instead, OVA could be seen within colonic epithelial cells, as well as within the lamina propria and occasionally in the submucosa. At high magnification, OVA could be seen localized between IECs as well as within IECs, suggesting it crosses the colonic epithelium through both paracellular and transcellular routes (Figure 3*B*, lower panel). These findings confirm that DSS-induced damage to the colonic epithelium enables orally gavaged

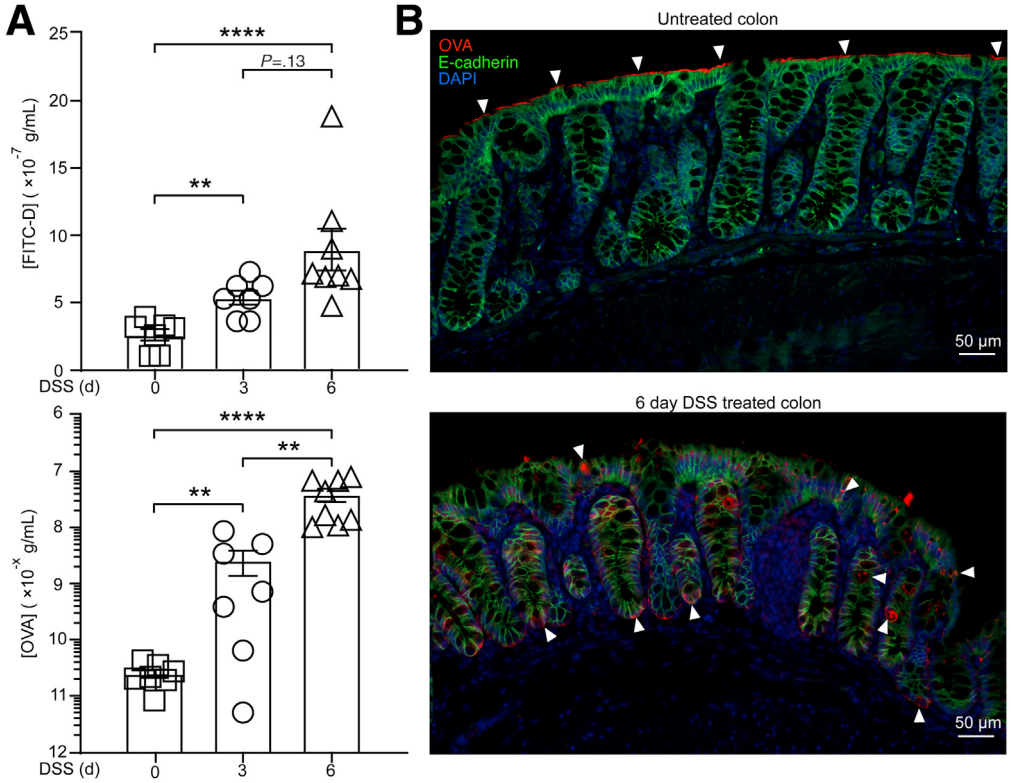

Figure 3. The OVA assay shows high sensitivity and specificity to detect intestinal barrier dysfunction in a mouse model of DSS-induced colitis. (*A*) OVA or FITC-D assay readouts from the plasma samples of nontreated (n = 8) or DSS-treated (n = 8) mice co-administered FITC-D (12 mg/mouse) and OVA (1 mg/mouse). Data presented are representative of at least 3 independent experiments. Statistical significance was determined by 1-way analysis of variance using the Tukey post hoc test. (*B*) Visualization of OVA localization in the distal colon of nontreated (*upper panel*) or DSS-treated for 6 days (*lower panel*) WT mice. Mice were orally gavaged with 1 mg/100 μL OVA and tissues were harvested 3 hours later for histology and stained with the same rabbit anti-OVA antibody used in the OVA assay. The localization of OVA (red) is highlighted with *white arrowheads*, along with stains for epithelium (E-cadherin, green), and nuclei (DAPI, blue). DAPI, 4′,6-diamidino-2-phenylindole. *$P \leq .05$, **$P \leq .01$, *** $P \leq .001$, **** $P \leq .0001$.

OVA to translocate across the epithelium in this model of colitis.

The OVA Assay Can Detect Subtle Permeability Defects in Mice With Impaired Mucus Structure/Function

Aside from the intestinal epithelium, the overlying colonic mucus layer also contributes to mucosal barrier function, both directly, as well as indirectly through the promotion of healthy IECs. Because formalin does not preserve the mucus layer effectively, to clarify whether mucus impacts the localization of OVA we stained colonic tissues fixed with Carnoy's fixative and found that, indeed, the majority of the OVA appeared to be segregated within the colonic lumen by the mucus layer (Figure 4*A*). These data suggest that under physiological conditions, the mucus layer also acts as a barrier to restrict OVA within the colonic lumen.

We and others have shown that when intestinal mucus is deficient (ie, *Muc2*$^{-/-}$ mice), gut barrier permeability is increased modestly, as assessed using the FITC-D method.[22–24] To directly compare the sensitivity of the OVA and FITC-D assays in measuring increases in barrier permeability owing to defects in mucus production, we bred heterozygous *Muc2*$^{+/-}$ mice to generate experimental *Muc2*$^{-/-}$ mice along with littermate *Muc2*$^{+/-}$ and *Muc2*$^{+/+}$ control mice.

Cohorts of 10- to 12-week-old female *Muc2*$^{+/+}$ (WT), *Muc2*$^{+/-}$, and *Muc2*$^{-/-}$ mice were gavaged with 100 μL PBS containing 120 mg/mL FITC-D and 10 mg/mL OVA. Cardiac puncture was performed 6 hours later to collect plasma for independent measurements of the respective probes. Although both methods showed increased plasma probe concentrations in *Muc2*$^{-/-}$ mice relative to WT (*Muc2*$^{+/+}$) mice, in a manner consistent with our previous report,[23] the FITC-D method only showed statistical significance, as assessed by 1-way analysis of variance, between *Muc2*$^{+/+}$ and *Muc2*$^{-/-}$ mouse strains (log transformed concentration of *Muc2*$^{+/+}$ vs *Muc2*$^{-/-}$, -6.37 ± 0.11 vs -6.04 ± 0.05; $P = .02$) (Figure 4*B*). By contrast, the same samples measured for OVA concentrations showed highly significant differences between all genotypes (log transformed concentration of *Muc2*$^{+/+}$ vs *Muc2*$^{+/-}$, -10.58 ± 0.06 vs -9.77 ± 0.24; $P = .05$; *Muc2*$^{+/+}$ vs *Muc2*$^{-/-}$, -10.58 ± 0.06 vs -8.06 ± 0.33; $P = .0002$; *Muc2*$^{+/-}$ vs *Muc2*$^{-/-}$, -9.77 ± 0.24 vs -8.06 ± 0.33; $P = .002$) (Figure 4*B*), indicating that loss of function of even 1 *Muc2* allele significantly weakens intestinal barrier function.

We next tested if the OVA assay could be used to measure intestinal permeability over a time course by repeatedly sampling the same mouse. This approach cannot be used humanely with the FITC-D assay because it requires a large blood volume (100–200 μL) that necessitates killing the test animal. To track intestinal permeability in *Muc2*$^{-/-}$ mice over a period of 5 days, cohorts of *Muc2*$^{-/-}$ mice were gavaged with 100 μL of 10 mg/mL OVA in PBS and 2.5 μL blood samples obtained from tail pokes performed at the indicated time points. As soon as the blood (OVA) readings neared baseline, we gavaged the animals again with the same amounts of OVA (1 mg/100 μL) and collected blood samples again as indicated. As shown in Figure 4*C*, we found that *Muc2*$^{-/-}$ mice within a single cage showed different degrees of intestinal permeability. This variation in intestinal permeability between mice likely reflects the stochastic nature of the spontaneous colitis that can slowly develop in these mice.[25] Interestingly, over the course of 5 days, the leakiness of each individual mouse relative to its cage mates remained the same as indicated by the order of symbols indicated by the 2 rectangular boxes in Figure 4*C*. Taken together, these data suggest that the OVA assay can detect subtle changes in intestinal permeability and can be tracked reliably within the same animal over time.

Notably, the Muc2 protein is heavily glycosylated, with as much as 80% of its weight comprising O-linked glycans,[26] through the actions of O-glycan branch forming core 1 β1,3 and core 3 β1,3-N glycosyltransferases (Figure 4*D*). Significantly, mice lacking functional core-1 or core-3 glycosyltransferases show thinner intestinal mucus layers, and those lacking the core 1 enzyme can develop spontaneous colitis by 4–6 months of age.[27] Even so, it is unclear whether these mice also show increased baseline intestinal permeability at time points before overt colitis development. To address this question using our OVA bead assay, we gavaged cohorts of 8- to 10-week-old IEC–core 1 β1,3-galactosyltransferase-deficient mice (*Villin*^{Cre}-*C1galt1*$^{-/-}$) and core 3 β1,3-N-acetylglucosaminyltransferase-deficient (*C3GnT*$^{-/-}$) mice with 1 mg OVA suspended in 100 μL PBS, and measured amounts of OVA translocated to the plasma as outlined earlier.

We found that IEC–*C1galt1*$^{-/-}$ mice showed increased intestinal permeability compared with their flox controls (*Core 1*$^{fl/fl}$) (Figure 4*E*), with the *C3GnT*$^{-/-}$ mice showing an intermediate phenotype (Figure 4*F*). Although the leakiness of their intestines was not as severe as what we had observed in *Muc2*$^{-/-}$ mice (500 times higher than WT [*Muc2*$^{+/+}$][18]), IEC–*C1galt1*$^{-/-}$ mice did show blood concentrations of OVA approximately 100-fold higher than seen in *C1galt1*$^{fl/fl}$ controls 6 hours postgavage (*C1galt1*$^{fl/fl}$ 4.0 × 10^{-11} vs IEC-*C1galt1*$^{-/-}$ 3.4 × 10^{-9} g/mL) (Figure 4*E*), whereas *C3GnT*$^{-/-}$ mice had approximately 60-fold higher levels of OVA in their plasma compared with their controls 6 hours postgavage (B6 6h 2.6 × 10^{-11} vs *C3GnT*$^{-/-}$ 1.6 × 10^{-9} g/mL) (Figure 4*F*). Interestingly, when the permeability of IEC–*C1galt1*$^{-/-}$ and *C3GnT*$^{-/-}$ mice were compared, they were found to be significantly different only at the 1-hour time point (Figure 4*G*), suggesting that although both enzymes play important roles in promoting mucus barrier function, the core 1 enzyme may play a larger role than core 3 in more proximal regions of the murine GI tract.

The OVA Assay Can Detect Increased Intestinal Permeability During Infectious Colitis

Enteric infections also can cause increases in intestinal permeability. Among the various mouse models of GI infection, we and others have shown that the attaching and effacing bacterial pathogen *Citrobacter rodentium* causes increased intestinal permeability[28,29] in concert with

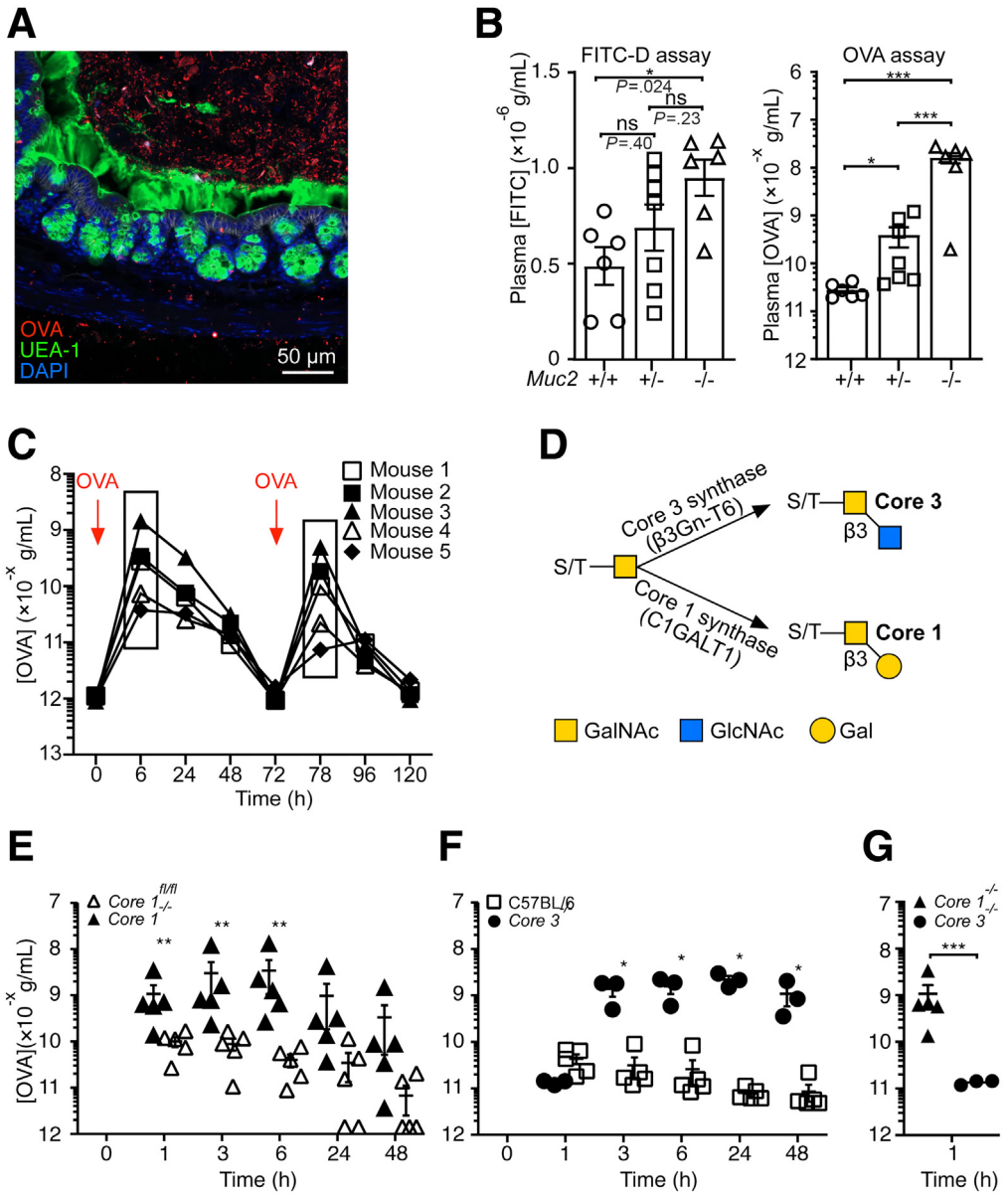

Figure 4. Muc2 and its glycosylation are critical for limiting OVA interactions with the intestinal epithelium and regulating intestinal permeability. (*A*) Visualization of OVA localization in the colon. Colonic tissue samples containing fecal matter from C57BL/6 mice were harvested and fixed with methyl-Carnoy's fixative, and then stained for OVA (red), fucosylated residues on mucins (Ulex Europaeus Agglutinin I [UEA-1] lectin, green), epithelial cells (E-cadherin, white), and nuclei (DAPI, blue). (*B*) OVA or FITC-D assay readouts form the plasma samples of *Muc2*$^{+/+}$ (WT) (n = 6), *Muc2*$^{+/-}$ (n = 7), and *Muc2*$^{-/-}$ mice (n = 6) co-administered OVA and FITC-D. Data are representative of at least 3 independent experiments. Statistical significance was determined by 1-way analysis of variance, using the Tukey post hoc test. (*C*) A cohort of 10-week-old female *Muc2*$^{-/-}$ mice (n = 5) was gavaged with 1 mg/mouse OVA as indicated and 2.5 μL blood samples were taken as indicated to track intestinal permeability changes within each animal. (*D*) Mechanistic actions of core 1 and core 3 synthases in the glycosylation of mucins. (*E*) Representative intestinal permeability data using the OVA assay on 8- to 10-week-old IEC–*C1galt1*$^{-/-}$ mice (n = 5) and (*F*) *C3GnT*$^{-/-}$ mice (n = 3) (denoted *Core 1*$^{-/-}$ and *Core 3*$^{-/-}$ mice, respectively) relative to control IEC–*C1galt1*$^{fl/fl}$ (*Core 1*$^{fl/fl}$) (n = 5) and C57BL/6 mice (n = 5). (*G*) Comparison of intestinal permeability from OVA assay readouts between IEC–*C1galt1*$^{-/-}$ and *C3GnT*$^{-/-}$ mice in panels *E* and *F* 1 hour after OVA gavage. Mice were gavaged with 1 mg/mouse OVA and 2.5 μL blood samples were taken at the indicated time points. Data are representative of 3 separate experiments. C1GALT1, core 1 β1,3-galactosyltransferase; DAPI, 4′,6-diamidino-2-phenylindole; Gal, galactose; GalNAc, N-acetylgalactosamine; GlcNAc, N-acetylglucosamine; S, serine; T, threonine; β3Gn-T6, β1,3-N-acetylglucosaminyltransferase 6. *$P \leq .05$, **$P \leq .01$, ***$P \leq .001$.

modest tissue pathology and inflammation. To test the applicability of the OVA assay to this model, C57BL/6 mice were infected with 2×10^8 CFU of *C rodentium* and gavaged with 100 μL of 10 mg/mL OVA on day 6 postinfection (pi). This is the earliest time point at which we previously have observed intestinal barrier dysfunction in this model.[30] At 6 hours postgavage, the mice blood samples were collected and assayed for the presence of OVA. We detected a statistically significant approximately 850-fold change in intestinal permeability within the same animals using the OVA assay, with baseline levels ($2.50 \pm 0.43 \times 10^{-11}$) increasing to $2.13 \pm 0.56 \times 10^{-8}$ on day 6 pi ($P = .0001$) (Figure 5*A*). These results suggest the OVA assay can detect subtle changes in intestinal permeability within the *C rodentium* infection model.

Attaching and effacing bacterial pathogens such as *C rodentium* cause IEC barrier disruption by adhering to the apical surface of IECs and translocating effector proteins into these cells through their type 3 secretion system.[31] To address the localization of *C rodentium* vs OVA in this system, we co-stained distal colon tissue sections with the anti-OVA antibody and with antisera against *Escherichia coli* lipopolysaccharide (Poly 8), which has been shown to recognize *C rodentium*,[32] which expresses one of the targeted O-antigens (O152). We readily detected *C rodentium* adherent to the colonic mucosal surface and frequently found OVA signal nearby, as well as penetrating deep into infected crypt lumens (Figure 5*B*, highlighted by arrowheads). These data confirm that *C rodentium* infection leads to barrier

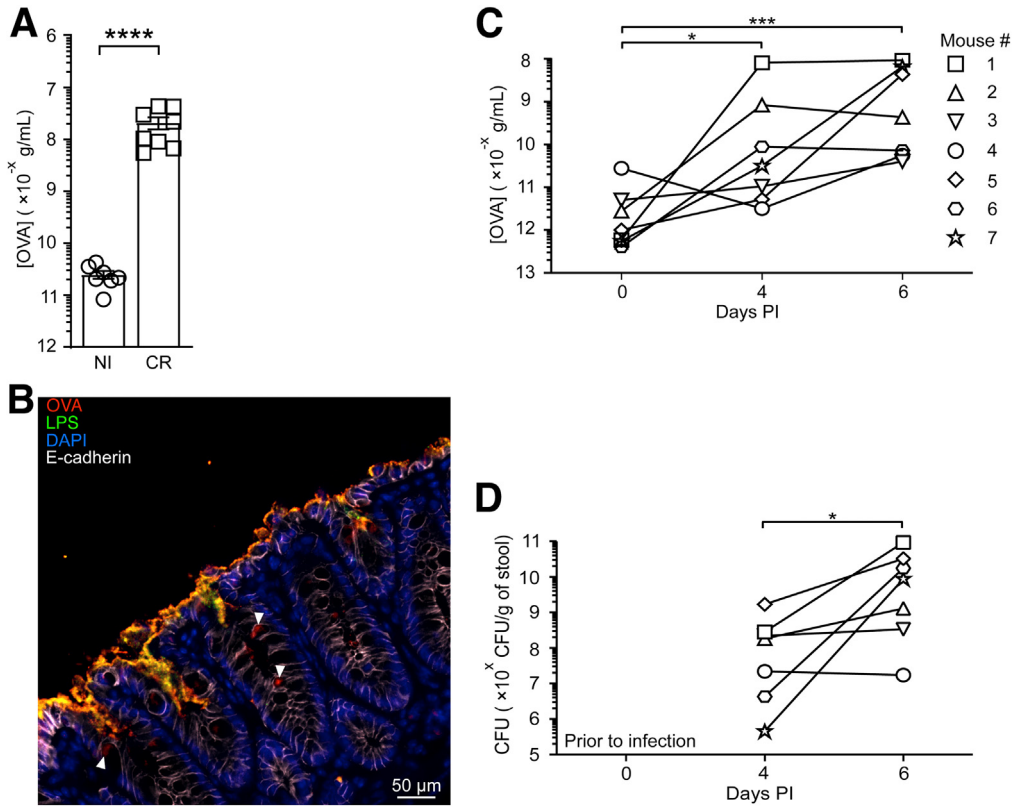

Figure 5. *C rodentium* infection of the GI tract causes lesions that allow OVA to penetrate across the intestinal epithelium. (*A*) Representative data on OVA assays of cohorts (n = 12) of 6- to 8-week-old *C rodentium*–infected (6 days pi) or –uninfected female WT C57BL/6 mice. Mice were gavaged with 1 mg OVA and blood samples were taken 6 hours postgavage. Data are representative of 3 separate experiments. A 2-tailed Student *t* test was used to determine the statistical significance. (*B*) Distal colon tissues from mice infected with *C rodentium* for 6 days were stained to identify OVA (red). OVA was detected near adherent *C rodentium* (green), as well as deep in heavily infected crypts (*arrowheads*), while E-cadherin (white) and DAPI (blue) also were stained. (*C*) Representative OVA assay data tracking intestinal permeability both before and during a course of *C rodentium* infection. Cohorts (n = 4) of numbered 6- to 8-week-old female C57BL/6 mice had the intestinal permeability OVA assay performed just before infection, and, subsequently, again on days 4 and 6 pi with *C rodentium*. To address the concern that any residual circulating OVA from an earlier OVA assay may affect the results, blood was sampled just before OVA gavage to establish pre-existing baselines, and these values then were subtracted from the day 6 readings. Results are representative of 3 independent experiments. Blood samples were taken 6 hours after OVA gavage (1 mg/mouse) on the indicated days pi. (*D*) Pathogen stool burdens of mice described in panel *C*. Mice were gavaged with OVA either before *C rodentium* infection (day 0), or on days 4 or 6 pi. Stool samples were collected immediately after gavage, while blood samples were collected 6 hours after OVA gavage. Stool samples were plated in triplicate on Luria broth agar plates containing 100 μg/mL streptomycin. Statistical significance for panels *C* and *D* were determined by 1-way analysis of variance using the Tukey post hoc test. CR, Citrobacter rodentium; DAPI, 4′,6-diamidino-2-phenylindole; NI, Not infected. *$P \leq .05$, ***$P \leq .001$, ****$P \leq .0001$.

disruption, allowing luminal factors (such as OVA) to enter colonic crypts and translocate across the epithelial barrier

Although we expect that intestinal permeability will increase as *C rodentium* infection progresses, researchers have been unable to track this in the same mice over a time course because the FITC-D and Ussing chamber approaches necessitate killing the mice. To test this hypothesis, we gavaged heathy mice with OVA, and, 6 hours later, 2.5 μL blood samples were tested using the OVA assay to establish a baseline. Subsequently, these mice were infected with 2×10^8 colony-forming units of *C rodentium* and gavaged with OVA on day 4 pi, going through the same procedure as described earlier, and then again on day 6 pi. As shown in Figure 5*C*, baseline blood OVA levels before infection were extremely low, but they showed a large statistically significant increase (~240-fold) when the assay was repeated on day 4 pi (day 0, $5.45 \pm 3.78 \times 10^{-12}$ vs day 4, $1.30 \pm 3.78 \times 10^{-9}$; $P < .0133$). By day 6 pi, after a new gavage of OVA, plasma OVA levels were increased further by another 2-fold ($2.98 \pm 3.78 \times 10^{-9}$; $P < .0002$). In addition, we observed that those mice with the highest *C rodentium* stool burdens (on days 4 or 6 pi), showed the highest intestinal permeability to OVA (Figure 5*D*). Thus, the OVA assay appears useful in assessing intestinal barrier dysfunction and disease (pathogen burden) during enteric infection and colitis.

Discussion

The FITC-D and Ussing chamber assays are the most common methods used by researchers to measure intestinal permeability in mice. The FITC-D assay is relatively simple to establish and offers reasonable sensitivity. Unfortunately, the blood volume typically needed for the assay (100–200 μL) requires the test animal to be killed, therefore providing only a snapshot of what is a highly dynamic process. Similarly, Ussing chambers can accurately measure intestinal permeability ex vivo, but also require the test animal to be killed. Moreover, the cost of the equipment, as well as its technical challenges, have reduced Ussing chamber use in recent years.

Although the OVA assay is a flow cytometry–based assay, and thus slightly more complex than the FITC-D assay, it still is relatively simple because it uses a single color (requiring no fluorescence compensation). Moreover, expertise in the use of flow cytometers is widespread in universities and research centers. Another feature is that the OVA assay uses a well-characterized antigen and therefore a large selection of OVA antibodies are available for further analysis. In terms of cost, the OVA assay is surprisingly cheap ($0.1/sample) compared with FITC-D ($5.45/sample), even with the cost of operating the flow cytometer factored in (Table 1). The most beneficial feature of the OVA assay is that it can be performed without killing the animal, allowing intestinal permeability to be tracked over an extended time period. Not only does this reduce experimental variation, but it also significantly can reduce the number of animals used in each experiment. In this report, we performed a series of benchmarking experiments to compare the background noise level, detection limit, and sensitivity of the OVA and FITC-D assays relative to one another in several mouse models of intestinal barrier dysfunction and/or colitis.

We first examined the detection limit of the respective assays by comparing the standard curves to determine their dynamic ranges. The dynamic range of the OVA assay is 6 orders of magnitude (ie, 10^{-6} to 10^{-12} g/mL) whereas the FITC-D assay covers 10^{-4} to 10^{-9} g/mL. Although differing by only 1 order of magnitude, the OVA assay is sensitive down to 10^{-12} g/mL, a level 1000-fold lower than that of the FITC-D assay. We posit that this enhanced sensitivity is owing to OVA being a large (45 kilodalton) protein,[33] carrying many different epitopes, thus allowing OVA to be effectively captured and bound by the 2 polyclonal anti-OVA antibodies. The epitopes contained in the rabbit polyclonal antibodies then are amplified further by the donkey anti-rabbit polyclonal antibody, generating a robust signal even at low concentrations. Next, we compared the background noise of the respective assays by obtaining a reading from the plasma of untreated C57BL/6 mice using the respective assays. We found that the background noise reading of the OVA assay is approximately 8 times above the lower detection limit whereas the FITC-D assay is roughly 35 times. This suggests that the OVA assay is more sensitive but also raises the question of why the background noise of the FITC-D assay is so high? We suspect the background signal may arise from components

Table 1. Cost Comparison Between the FITC-D and OVA Assays

Component (Manufacturer)	Unit price	Number of tests per unit	Cost per test
5-μm CML beads (ThermoFisher)	$461	3.6×10^5	$0.001
Goat anti-OVA antibody (MP Biomedicals)	$240	4.5×10^4	$0.005
Rabbit anti-OVA antibody (Bethyl Laboratory)	$122	2000	$0.06
PE anti-rabbit antibody (Jackson Immunoresearch Laboratories)	$255	10,000	$0.03
Total			$0.1
FITC-D (Sigma)	$452	83	$5.4
Total			$5.4

NOTE. Beads generated per conjugation reaction, 1.80×10^7; number of beads used per test, 20,000; and number of tests per conjugation reaction, 900.

of the plasma, which is known to contain biological molecules excitable by the same wavelength of light used to excite the FITC-D molecules.[34]

We began our benchmarking experiment with the DSS colitis model by co-administering OVA and FITC-D to C57BL/6 mice provided drinking water containing DSS for 3 or 6 days. We found that in healthy mice there was very little OVA detected in their plasma, suggesting that very modest levels of OVA cross the intact epithelial barrier. This was corroborated by the immunostaining of intestinal sections of control mice, where OVA could be seen in the cecal and colonic lumen and lining the epithelial surface, but none detectable penetrating the epithelium. In the DSS-treated mice, both assays were able to detect increased permeability on day 3 post-DSS, however, the sensitivity was dramatically different. Despite the overt colonic pathology, the FITC-D assay showed only a 2-fold increase in intestinal permeability after 3 days of DSS treatment, and another 2-fold increase from day 3 to day 6. In contrast, the OVA assay showed a 100-fold increase from baseline after 3 days of DSS and another 15-fold increase (1500-fold higher than before DSS) from day 3 to day 6. These results suggest that the OVA assay has superior resolving power compared with the FITC-D assay.

A defective mucus barrier is a defining feature of IBD[27] as well as most murine IBD models, although its impact on intestinal permeability is poorly defined.[35] Therefore, we performed additional benchmarking experiments using mouse strains suffering varying degrees of structural/functional impairment of their mucus barrier. It has been shown previously that the severity of DSS colitis in mice is correlated negatively to their copy number of Muc2 genes (ie, *Muc2*$^{+/+}$ mice develop mild colitis, *Muc2*$^{+/-}$ mice develop moderate colitis, and *Muc2*$^{-/-}$ mice develop severe colitis).[25] Whether the heightened susceptibility of *Muc2*$^{+/-}$ mice to DSS is associated with impaired baseline barrier function was unknown. To test this hypothesis, we co-administered OVA and FITC-D to *Muc2*$^{+/+}$, *Muc2*$^{+/-}$, and *Muc2*$^{-/-}$ mice and found their intestinal permeability correlated with the number of functional *Muc2* alleles. Notably, we observed statistically significant differences using the OVA assay, but not with the FITC-D assay. Our results were consistent with our previous findings that the intestinal permeability of *Muc2*$^{-/-}$ mice was increased,[22] although with the OVA assay, we identified a 600-fold increase in permeability over that of *Muc2*$^{+/+}$ mice. Moreover, we also discerned a 14-fold higher level of OVA in the plasma of *Muc2*$^{+/-}$ mice compared with WT *Muc2*$^{+/+}$ mice.

Because intestinal permeability under disease conditions could be dynamic, being able to repeatedly sample an individual could prove highly informative. Taking advantage of the ability to sample several small volumes of blood from the same animal, we investigated the intestinal permeability of *Muc2*$^{-/-}$ mice over the course of a week by repeatedly gavaging and sampling the same mice. We found that over the week, the intestinal permeability of a given cohort of *Muc2*$^{-/-}$ mice remained fairly consistent, showing the reliability of the assay. Given that we could detect a significant difference in intestinal permeability between the *Muc2*$^{+/+}$ and *Muc2*$^{+/-}$ mice, we speculated that other defects in mucus structure or function also could lead to increased intestinal permeability, and sought to test this using the OVA assay. As previously noted, the core 1 and core 3 glycosyltransferases are important for properly glycosylating O-linked glycans of the Muc2 mucin, with their loss rendering a host more susceptible to chemically induced or spontaneous colitis.[36–39] We found that both IEC–*C1galt1*$^{-/-}$ and *C3GnT*$^{-/-}$ mice showed significantly increased permeability when compared with their WT controls using the OVA assay. These results illustrate the importance of the intestinal mucus and its appropriate glycosylation in regulating intestinal permeability. Furthermore, our study also highlights the utility of the OVA assay in detecting more subtle changes in barrier function.

Lastly, we investigated whether the OVA assay has utility in tracking barrier function in the *C rodentium* infection model because this is a well-established model in which barrier disruption has been shown using the FITC-D assay. Using the OVA assay, we showed that *C rodentium* infection increased intestinal permeability by 850-fold above baseline on day 6 pi. Moreover, we were able to assess intestinal permeability over a time course of infection, showing within the same mice that barrier dysfunction was increased drastically over baseline by day 4 pi, and further increased at day 6 pi. Thus, by using the OVA assay, we can study changes in intestinal permeability as they develop through the course of disease, and potentially into recovery.

A possible caveat to repeated OVA assays (ie, repeated OVA oral gavages) is its potential to elicit an immune response resulting in the production of autologous anti-OVA antibodies, which may impede the capture and detection antibodies used in the assay. Because host blocking antibodies may be a complication with the repeated administration of any antigen, it may be necessary to use a variety of probes to assess barrier function in longer-term studies. In this same vein, we previously showed that bovine β-lactoglobulin also could be used as a probe to track intestinal permeability in *Muc2*$^{-/-}$ mice.[18] Given the potential for host antiprobe antibodies to confound results, we suggest caution when using the same probe for experiments lasting longer than a week and testing for probe-specific adaptive immune responses. For extended studies, exploring the use of synthetic molecules that are comparatively less immunogenic yet show similar chemical and physical properties as OVA or β-lactoglobulin is suggested. Such probes would permit repeated permeability readings for a longer period of time without the interference of autologous antibodies.

Although the current study focuses on mouse models, intestinal permeability also significantly is increased in patients with IBD. Whether a causal relationship exists is unclear, however, increased permeability has been associated strongly with increased susceptibility to IBD,[3] its disease activity,[4–7] as well as susceptibility to other autoimmune and autoinflammatory disorders.[8–10] The lactulose mannitol (LM) test is the clinical gold standard for measuring intestinal permeability in patients suffering conditions involving barrier dysfunction.[11] The LM test is performed in fasted patients who drink a solution containing defined amounts of

the 2 nonmetabolizable sugars. Urine samples then are collected and analyzed for the presence of the sugars. Patients undertaking the LM test are confined to the testing facility, limiting its attractiveness to patients and clinicians. The OVA assay may prove a potential alternative to the LM test, given that the assay requires a very small volume of blood to perform. Moreover, the finger prick procedure is safe, easy, and relatively painless, while food-grade, pasteurized ovalbumin is cheap and readily available. We also will assess whether ovalbumin can be detected after the consumption of eggs, or egg-containing foods such as baked goods. In addition, we also have shown that increases in intestinal permeability can be monitored by quantitating OVA in urine.[18] Moreover, this alternative sampling approach may prove valuable for widespread adoption in the clinic given that many young patients suffer from needle phobia. Moreover, there is no need for test subjects to be confined for the duration of the test. We will explore this possibility by investigating the safety profile and clinical utility of the OVA assay to pave the way for its translation into clinical use.

Material and Methods

Mice

The IEC-specific *C1galt1* deficient (IEC–*C1galt1*$^{-/-}$) mice were generated by crossing the *C1galt1*–flox mice with *Villin*^{Cre} mice as previously described.[40] The core 3 transferase-deficient (*C3GnT*$^{-/-}$), C57BL/6, and *Muc2*$^{-/-}$ mice[41] were bred under specific pathogen-free and *Helicobacter*-free conditions at British Columbia Children's Hospital Research Institute. Both male and female mice were used in the experiments unless specified. To ensure age and sex were consistent in the DSS and *C rodentium* infection experiments, female C57BL/6 mice also were purchased from the Jackson Laboratory. All experiments were conducted in accordance with the protocols and guidelines approved by the Animal Care Committee at the University of British Columbia and Canadian Council on Animal Care.

Preparation of Ovalbumin-Specific CML Beads for the OVA Assay

The anti-OVA polyclonal antibodies were conjugated to CML (#C37255; ThermoFisher) beads using the carbodiimide method as previously described.[42,43] The 2-(N-morpholino) ethanesulfonic acid (MES) buffer and the 1-ethyl-3-(3-dimethylaminopropyl) carbodiimide (EDAC) were prepared immediately before the conjugating reaction to ensure maximum activity. To prepare the MES buffer, MES was first dissolved in distilled H_2O. EDTA was added to create a buffer with a final concentrations of 50 mmol/L MES and 1 mmol/L EDTA, with the pH adjusted to 6.0. The EDAC powder was first weighed in a 15-mL conical tube (0.01–0.015 g) and dissolved in sufficient MES buffer for the EDAC–MES solution to have a final concentration of 50 mg/mL.

To prepare the CML beads, 5 beads were first resuspended by vortexing at maximum speed for 1 minute. Several drops of the beads were transferred into a 1.5-mL Lobind Eppendorf tube (#0030108442; Eppendorf). The beads were pelleted by centrifugation at 15,000 $\times$ *g* for 3 minutes at room temperature. The supernatant was removed by careful aspiration using a pipette. The CML beads were washed with 500 μL PBS 2–3 times and finally resuspended in 100 μL MES buffer by pipetting. A 10-μL aliquot of the CML beads was diluted 5000–10,000 times using PBS for enumeration on a hemocytometer. After the bead concentration was determined, 1.8 $\times$ 10^7 CML beads were transferred into a 1.5-mL Lobind Eppendorf tube and increased to a 50μL volume using the MES buffer. The CML beads were activated by adding 20 μL EDAC–MES solution, mixed by pipetting and placed on a shaker set at 800 RPM for 15 minutes at room temperature to ensure the beads did not settle. Alternatively, the beads could be kept suspended by pipetting every 1–2 minutes if a shaker was not available. After 15 minutes of activation, the CML beads were pelleted by centrifugation at 15,000 $\times$ *g* for 3 minutes at room temperature followed by two–three 500 μL PBS washes. The CML beads were pelleted by centrifugation, PBS was removed by careful aspiration, and the beads were ready for antibody conjugation.

To conjugate the antibody to the beads, activated CML beads were resuspended in 100 μL goat anti-OVA polyclonal antibodies (#0855303; MP Biomedicals) and incubated on a shaker set at 800 RPM for 4 hours at room temperature. The CML beads were pelleted at 15,000 $\times$ *g* after incubation, washed 2–3 times with 500 μL PBS, and resuspended in 100 μL Quenching, Blocking, and Storage buffer (1% bovine serum albumin, 0.02% NaN_3 in PBS) to inactivate any remaining chemical groups on the bead surfaces. The CML beads were enumerated and stored at 4°C for up to 6 months. Bead activity should be checked every month to ensure reliable results are obtained. It should be noted that the antibody concentrations (rabbit and goat anti-OVA and donkey anti-rabbit Phycoerythrin [PE]) described in this study were optimized empirically using serially diluted antibodies and ovalbumin. Should the end user decide to use other preparations of anti-ovalbumin antibodies and/or detection antibodies, optimization experiments are strongly recommended.

Measurement of Intestinal Permeability Using FITC-D

FITC-D (#68059; Sigma-Aldrich) was dissolved in either sterile PBS or PBS containing 10 mg/mL OVA (for co-administration experiments) to a working concentration of 120 mg/mL. Each mouse was given 100 μL FITC-D solution via oral gavage (12 mg per mouse). Animals were fasted for the duration of the assay and killed 6 hours later by cervical dislocation, and blood samples were collected using cardiac puncture. Plasma was isolated using centrifugation and the plasma concentration of FITC-D was measured using a fluorimeter (ThermoFisher Scientific).

Measurement of Intestinal Permeability Using the OVA Assay

Buffer (1$\times$ PBS, 2% heat inactivated fetal bovine serum, 2 mmol/L EDTA, and 0.05% Tween 20) (FACST) was freshly

prepared before the assay. To detect the presence of OVA in mouse blood, 2.5- to 5-μL aliquots of blood were collected using heparinized microhematocrit capillary tubes (Fisher) using the tail poke technique illustrated in Figure 1. Blood samples were mixed with 10 μL PBS containing 0.5% TWEEN 20 and 50 mmol/L EDTA for antigen linearization. Blood samples could be stored at -20°C while samples at other time points were collected. Samples could be stored at -20°C for up to 2 weeks. After sample collection was complete, blood samples were thawed at room temperature for 5 minutes, topped up to 100 μL with FACST buffer, and centrifuged at 2000 $\times$ g at 4°C for 3 minutes to pellet cell debris. Supernatants were aspirated carefully, transferred into 96-well U-bottom plates (BD Falcon), and 20,000 CML beads suspended in 10 μL FACST buffer were added into each of the wells and mixed by pipetting using a multichannel pipette.

Samples were incubated overnight on a plate shaker set at 800 rpm and 4°C. The next morning, CML beads were pelleted at 750 $\times$ g for 5 minutes at 4°C and the supernatant was removed. Rabbit anti-ovalbumin polyclonal antibody (100 μL, #GTX21221; GeneTex) diluted in FACST buffer (10 μg/mL final concentration) was added into each well and mixed using a multichannel pipette. The plate was incubated at room temperature on a plate shaker set at 800 rpm for 1.5–2 hours. After incubation, beads were pelleted by centrifugation at 750 $\times$ g for 5 minutes at 4°C and the supernatant was removed. The beads were stained with 100 μL PE conjugated-F(ab')$_2$ fragment donkey anti-rabbit IgG polyclonal antibody (#711-116-152; Jackson Immunoresearch Laboratories) that has minimal cross-reactive antibodies against IgG of various species including human beings, mice, rats, hamsters, and sheep. Subsequently, the secondary antibody was diluted in FACST buffer to a final concentration of 0.5 μg/mL and mixed by pipetting using a multichannel pipette. The plate was wrapped in tinfoil to protect it from light and incubated at room temperature on a plate shaker set at 800 rpm for 15 minutes. The beads were pelleted after incubation by centrifugation at 750 $\times$ g for 5 minutes at 4°C and the supernatant was removed, washed once with 200 μL FACST buffer, and resuspended in 200 μL FACST buffer for data acquisition. Data were acquired using BD Fortessa or BD LSR II flow cytometers in conjunction with BD FACSDiva software (BD Biosciences) as soon as the staining was complete, and analyzed using FlowJo software (FlowJo, LLC).

Tissue Processing and Immunostaining

For formalin-fixed sections, harvested tissue samples were fixed in buffered 10% formalin solution (#HT501128-4L; Sigma-Aldrich) at 4°C overnight before being transferred into 70% ethanol for paraffin embedding and sectioning. For mucus staining, harvested tissues were fixed in methacarn (60% methanol, 30% chloroform, and 10% glacial acetic acid) at 4°C for 1 hour before transfer into 100% methanol for embedding and sectioning.

For immunostaining, sections were deparaffinized by heating to approximately 60°C for 15 minutes, cleared with xylene, rehydrated through a decreasing ethanol gradient to water, steamed for 30 minutes in buffer (10 mmol/L sodium citrate, 0.05% Tween 20, pH 6.0) for antigen retrieval, and blocked with blocking buffer (donkey serum in PBS, containing 1% bovine serum albumin, 0.1% Triton X-100 [Sigma Alderich], 0.05% Tween 20 [Sigma Alderich], and 0.05% sodium azide) for 1 hour. For visualizing of OVA crossing the IEC barrier, rabbit anti-OVA polyclonal antibody (#GTX21221, 1:1000; GeneTex) or goat anti-OVA polyclonal antibody (#0855303, 1:100; MP Biomedicals) and mouse monoclonal anti-mouse E-cadherin antibody (#610182, 1:400; BD Transduction Laboratories) were used. APC-conjugated–F(ab')$_2$ fragment donkey anti-rabbit IgG polyclonal antibody (#711-116-152; Jackson Immunoresearch Laboratories), donkey AlexaFluor 568–conjugated anti-goat IgG (H+L) high cross-adsorbed secondary antibody (#A-11057; Thermal Fisher), and AlexaFluor 488–conjugated anti-mouse IgG (H+L) high cross-adsorbed secondary antibody (#R37114; Thermal Fisher) at a concentration of 1:2000 each. For the visualization of Muc2, antigen-retrieved and blocked slides were stained with FITC-conjugated Ulex Europaeus Agglutinin I (#FL-1061-5; Vector Laboratories) was used in a concentration of 1:2000). For the visualization of *C rodentium*, an antisera that previously has been shown to recognize *E coli* O152, the same O-antigen expressed on *C rodentium*[32] was used at a concentration of 1:1000 (#81449; SSI Diagnostica).

DSS Salt in Drinking Water Administration

DSS salt (#160110; MP Biomedicals) was dissolved in drinking water to generate a 3% (w/v) DSS solution. Mice were provided DSS drinking water exclusively for the indicated periods of time. Weight and stool consistency were monitored daily for clinical signs of colitis.

C rodentium *Infection*

A frozen stock of *C rodentium* biotype 4280 strain DBS100 (ATCC 51459; American Type Culture Collection, Manassas, VA) was streaked onto a Luria broth agar plate and a colony was used to inoculate an overnight culture into Luria broth at 37°C. On the day of the infection, 6- to 8-week-old female C57BL/6 mice were orally gavaged with 100 μL overnight culture containing approximately 2.5 $\times$ 10^8 colony-forming units of *C rodentium*. Mice were monitored for 6 days after the infection and the OVA assay was performed on the infected mice on day 6 pi.

Pathogen Burden Assessment of C rodentium *Infection*

Stool samples were collected immediately after OVA was gavaged and solubilized in 1 mL sterile PBS using a vortexer. Samples were serially diluted in sterile PBS and plated onto Luria broth agar plates containing 100 μg/mL streptomycin in triplicate. The agar plates were incubated at 37°C overnight and colonies were enumerated to assess pathogen burden.

Curve Fitting and Statistical Analyses

Statistical significance determination, standard curve fitting, and correlative analysis was performed using GraphPad Prism 6 software. Data were first tested with normality to determine whether parametric or nonparametric tests were required. Statistical significance was determined by unpaired, 2-tailed Student *t* tests or 1-way analysis of variance tests. The Tukey or Bonferroni methods were used as post hoc tests. A *P* value of .05 or less was considered significant, with asterisks denoting significance in the figures. Details on which statistical test and post hoc tests were used are indicated in the Figure legends.

References

1. Johansson ME, Hansson GC. Immunological aspects of intestinal mucus and mucins. Nat Rev Immunol 2016; 16:639–649.
2. de Souza HS, Fiocchi C. Immunopathogenesis of IBD: current state of the art. Nat Rev Gastroenterol Hepatol 2016;13:13–27.
3. Turner JR. Intestinal mucosal barrier function in health and disease. Nat Rev Immunol 2009;9:799–809.
4. González-González M, Díaz-Zepeda C, Eyzaguirre-Velásquez J, González-Arancibia C, Bravo JA, Julio-Pieper M. Investigating gut permeability in animal models of disease. Front Physiol 2018;9:1962.
5. Accarie A, Vanuytsel T. Animal models for functional gastrointestinal disorders. Front Psychiatry 2020;11: 509681.
6. Galipeau HJ, Verdu EF. The complex task of measuring intestinal permeability in basic and clinical science. Neurogastroenterol Motil 2016;28:957–965.
7. Turpin W, Lee SH, Raygoza Garay JA, Madsen KL, Meddings JB, Bedrani L, Power N, Espin-Garcia O, Xu W, Smith MI, Griffiths AM, Moayyedi P, Turner D, Seidman EG, Steinhart AH, Marshall JK, Jacobson K, Mack D, Huynh H, Bernstein CN, Paterson AD, Croitoru K. Crohn's and Colitis Canada Genetic Environmental Microbial Project Research Consortium; CCC GEM Project recruitment site directors include Maria Abreu; Kenneth Croitoru. Increased intestinal permeability is associated with later development of Crohn's disease. Gastroenterology 2020;159:2092–2100.e5.
8. Buisine MP, Desreumaux P, Debailleul V, Gambiez L, Geboes K, Ectors N, Delescaut MP, Degand P, Aubert JP, Colombel JF, Porchet N. Abnormalities in mucin gene expression in Crohn's disease. Inflamm Bowel Dis 1999;5:24–32.
9. Johansson ME, Gustafsson JK, Holmén-Larsson J, Jabbar KS, Xia L, Xu H, Ghishan FK, Carvalho FA, Gewirtz AT, Sjövall H, Hansson GC. Bacteria penetrate the normally impenetrable inner colon mucus layer in both murine colitis models and patients with ulcerative colitis. Gut 2014;63:281–291.
10. Bjarnason I, O'Morain C, Levi AJ, Peters TJ. Absorption of 51chromium-labeled ethylenediaminetetraacetate in inflammatory bowel disease. Gastroenterology 1983; 85:318–322.
11. Wyatt J, Vogelsang H, Hübl W, Waldhöer T, Lochs H. Intestinal permeability and the prediction of relapse in Crohn's disease. Lancet 1993;341:1437–1439.
12. Mu Q, Kirby J, Reilly CM, Luo XM. Leaky gut as a danger signal for autoimmune diseases. Front Immunol 2017; 8:598.
13. Buscarinu MC, Cerasoli B, Annibali V, Policano C, Lionetto L, Capi M, Mechelli R, Romano S, Fornasiero A, Mattei G, Piras E, Angelini DF, Battistini L, Simmaco M, Umeton R, Salvetti M, Ristori G. Altered intestinal permeability in patients with relapsing-remitting multiple sclerosis: a pilot study. Mult Scler 2017;23:442–446.
14. Bjarnason I, Williams P, So A, Zanelli GD, Levi AJ, Gumpel JM, Peters TJ, Ansell B. Intestinal permeability and inflammation in rheumatoid arthritis: effects of non-steroidal anti-inflammatory drugs. Lancet 1984;2:1171–1174.
15. Clarke LL. A guide to Ussing chamber studies of mouse intestine. Am J Physiol Gastrointest Liver Physiol 2009; 296:G1151–G1166.
16. Bischoff SC, Barbara G, Buurman W, Ockhuizen T, Schulzke JD, Serino M, Tilg H, Watson A, Wells JM. Intestinal permeability–a new target for disease prevention and therapy. BMC Gastroenterol 2014;14:189.
17. Gordon M, MacDonald JK, Parker CE, Akobeng AK, Thomas AG. Osmotic and stimulant laxatives for the management of childhood constipation. Cochrane Database Syst Rev 2016;8:CD009118.
18. Tsai K, Huang YH, Ma C, Baldwin TA, Harder KW, Vallance BA, Priatel JJ. Cutting edge: intestinal mucus limits the clonal deletion of developing T cells specific for an oral antigen. J Immunol 2020;205:329–334.
19. Johansson ME, Gustafsson JK, Sjöberg KE, Petersson J, Holm L, Sjövall H, Hansson GC. Bacteria penetrate the inner mucus layer before inflammation in the dextran sulfate colitis model. PLoS One 2010;5:e12238.
20. Chassaing B, Aitken JD, Malleshappa M, Vijay-Kumar M. Dextran sulfate sodium (DSS)-induced colitis in mice. Curr Protoc Immunol 2014;104:15.25.1–15.25.14.
21. Cochran KE, Lamson NG, Whitehead KA. Expanding the utility of the dextran sulfate sodium (DSS) mouse model to induce a clinically relevant loss of intestinal barrier function. PeerJ 2020;8:e8681.
22. Zarepour M, Bhullar K, Montero M, Ma C, Huang T, Velcich A, Xia L, Vallance BA. The mucin Muc2 limits pathogen burdens and epithelial barrier dysfunction during Salmonella enterica serovar Typhimurium colitis. Infect Immun 2013;81:3672–3683.
23. Bergstrom KS, Kissoon-Singh V, Gibson DL, Ma C, Montero M, Sham HP, Ryz N, Huang T, Velcich A, Finlay BB, Chadee K, Vallance BA. Muc2 protects against lethal infectious colitis by disassociating pathogenic and commensal bacteria from the colonic mucosa. PLoS Pathog 2010;6:e1000902.
24. Borisova MA, Achasova KM, Morozova KN, Andreyeva EN, Litvinova EA, Ogienko AA, Morozova MV, Berkaeva MB, Kiseleva E, Kozhevnikova EN. Mucin-2 knockout is a model of intercellular junction defects, mitochondrial damage and ATP depletion in the intestinal epithelium. Sci Rep 2020;10:21135.

25. Van der Sluis M, De Koning BA, De Bruijn AC, Velcich A, Meijerink JP, Van Goudoever JB, Büller HA, Dekker J, Van Seuningen I, Renes IB, Einerhand AW. Muc2-deficient mice spontaneously develop colitis, indicating that MUC2 is critical for colonic protection. Gastroenterology 2006;131:117–129.
26. Johansson ME. Mucus layers in inflammatory bowel disease. Inflamm Bowel Dis 2014;20:2124–2131.
27. Theodoratou E, Campbell H, Ventham NT, Kolarich D, Pučić-Baković M, Zoldoš V, Fernandes D, Pemberton IK, Rudan I, Kennedy NA, Wuhrer M, Nimmo E, Annese V, McGovern DP, Satsangi J, Lauc G. The role of glycosylation in IBD. Nat Rev Gastroenterol Hepatol 2014;11:588–600.
28. Bhinder G, Sham HP, Chan JM, Morampudi V, Jacobson K, Vallance BA. The Citrobacter rodentium mouse model: studying pathogen and host contributions to infectious colitis. J Vis Exp 2013;72:e50222.
29. Lee AS, Gibson DL, Zhang Y, Sham HP, Vallance BA, Dutz JP. Gut barrier disruption by an enteric bacterial pathogen accelerates insulitis in NOD mice. Diabetologia 2010;53:741–748.
30. Gibson DL, Ma C, Bergstrom KS, Huang JT, Man C, Vallance BA. MyD88 signalling plays a critical role in host defence by controlling pathogen burden and promoting epithelial cell homeostasis during Citrobacter rodentium-induced colitis. Cell Microbiol 2008;10:618–631.
31. Bhavsar AP, Guttman JA, Finlay BB. Manipulation of host-cell pathways by bacterial pathogens. Nature 2007;449:827–834.
32. Vallance BA, Deng W, Knodler LA, Finlay BB. Mice lacking T and B lymphocytes develop transient colitis and crypt hyperplasia yet suffer impaired bacterial clearance during Citrobacter rodentium infection. Infect Immun 2002;70:2070–2081.
33. Huntington JA, Stein PE. Structure and properties of ovalbumin. J Chromatogr B Biomed Sci Appl 2001;756:189–198.
34. Atkins CG, Buckley K, Blades MW, Turner RFB. Raman spectroscopy of blood and blood components. Appl Spectrosc 2017;71:767–793.
35. Vancamelbeke M, Vermeire S. The intestinal barrier: a fundamental role in health and disease. Expert Rev Gastroenterol Hepatol 2017;11:821–834.
36. Bergstrom K, Fu J, Johansson ME, Liu X, Gao N, Wu Q, Song J, McDaniel JM, McGee S, Chen W, Braun J, Hansson GC, Xia L. Core 1- and 3-derived O-glycans collectively maintain the colonic mucus barrier and protect against spontaneous colitis in mice. Mucosal Immunol 2017;10:91–103.
37. Larsson JM, Karlsson H, Crespo JG, Johansson ME, Eklund L, Sjövall H, Hansson GC. Altered O-glycosylation profile of MUC2 mucin occurs in active ulcerative colitis and is associated with increased inflammation. Inflamm Bowel Dis 2011;17:2299–2307.
38. An G, Wei B, Xia B, McDaniel JM, Ju T, Cummings RD, Braun J, Xia L. Increased susceptibility to colitis and colorectal tumors in mice lacking core 3-derived O-glycans. J Exp Med 2007;204:1417–1429.
39. Xia L. Core 3-derived O-glycans are essential for intestinal mucus barrier function. Methods Enzymol 2010;479:123–141.
40. Fu J, Wei B, Wen T, Johansson ME, Liu X, Bradford E, Thomsson KA, McGee S, Mansour L, Tong M, McDaniel JM, Sferra TJ, Turner JR, Chen H, Hansson GC, Braun J, Xia L. Loss of intestinal core 1-derived O-glycans causes spontaneous colitis in mice. J Clin Invest 2011;121:1657–1666.
41. Velcich A, Yang WC, Heyer J, Fragale A, Nicholas C, Viani S, Kucherlapati R, Lipkin M, Yang K, Augenlicht L. Colorectal cancer in mice genetically deficient in the mucin Muc2. Science 2002;295:1726–1729.
42. Schrum AG, Gil D, Dopfer EP, Wiest DL, Turka LA, Schamel WW, Palmer E. High-sensitivity detection and quantitative analysis of native protein-protein interactions and multiprotein complexes by flow cytometry. Sci STKE 2007;2007:pl2.
43. Southwell AL, Smith SE, Davis TR, Caron NS, Villanueva EB, Xie Y, Collins JA, Ye ML, Sturrock A, Leavitt BR, Schrum AG, Hayden MR. Ultrasensitive measurement of huntingtin protein in cerebrospinal fluid demonstrates increase with Huntington disease stage and decrease following brain huntingtin suppression. Sci Rep 2015;5:12166.

Received June 22, 2022. Accepted October 7, 2022.

Correspondence
Address correspondence to: Bruce A. Vallance, PhD, British Columbia Children's Hospital Research Institute, Ambulatory Care Building, Room K4-188, 4480 Oak Street, Vancouver, British Columbia, Canada V6H 3V4. e-mail: bvallance@cw.bc.ca.

CRediT Authorship Contributions

Bruce Vallance (Conceptualization: Equal; Funding acquisition: Lead; Methodology: Equal; Project administration: Lead; Resources: Lead; Supervision: Lead; Writing – review & editing: Lead)

Kevin Tsai (Conceptualization: Lead; Data curation: Lead; Formal analysis: Lead; Investigation: Lead; Methodology: Lead; Writing – original draft: Lead; Writing – review & editing: Equal)

Caixia Ma (Methodology: Equal)

Xiao Han (Methodology: Supporting; Writing – review & editing: Supporting)

Joannie Allaire (Methodology: Supporting; Writing – review & editing: Equal)

Genelle R. Lunken (Methodology: Supporting; Writing – review & editing: Equal)

Shauna M. Crowley (Methodology: Supporting)

Hongbing Yu (Writing – review & editing: Equal)

Kevan Jacobson (Writing – review & editing: Supporting)

Lijun Xia (Resources: Supporting; Writing – review & editing: Supporting)

John J. Priatel (Conceptualization: Lead; Investigation: Equal; Methodology: Equal; Resources: Supporting; Supervision: Supporting; Writing – review & editing: Equal)

Conflicts of interest
The authors disclose no conflicts.

Funding
This study was supported by discovery grant 2018-05120 from the Natural Sciences and Engineering Research Council, operating grants PJT-159528 and 178090 from the Canadian Institutes of Health Research, and by the Crohn's and Colitis Canada (B.A.V.).